

Control of Particle Size Distribution in an Emulsion Copolymerization Reactor Via Cascade Regulation of Nucleation and Growth

Mustafa T. Dokucu and Francis J. Doyle¹

Department of Chemical Engineering
University of California Santa Barbara
Santa Barbara, CA 93106-5080

Key Words: PBE system, emulsion polymerization, control of PSD, cascade, nucleation, growth

Prepared for Presentation at the 2006 Annual Meeting, San Francisco, CA, Nov. 12-17
Copyright © 2006 M. T. Dokucu and F. J. Doyle III, University of California Santa Barbara

November 2006
Unpublished

AICHE shall not be responsible for statements or opinions contained in papers or in its publications.

¹ Author to whom correspondence should be addressed: doyle@enr.ucsb.edu

CONTROL OF PARTICLE SIZE DISTRIBUTION IN AN EMULSION COPOLYMERIZATION REACTOR VIA CASCADE REGULATION OF GROWTH AND NUCLEATION

Mustafa T. Dokucu, Francis J. Doyle III

University of California Santa Barbara, Santa Barbara, CA

Introduction

Emulsion polymerization has significant advantages over bulk and solution polymerization processes. These advantages result mostly from the multiphase and compartmentalized nature of the emulsion polymerization, delivering a high versatility to product qualities but adding to the complexity of the process. The control of the full particle-size distribution (PSD) in emulsion polymerization is vital for industrial applications where the target distributions are usually complex and/or multimodal. In these cases, end-use properties (mechanical, rheological, optical) of the polymer products depend strongly on the endpoint PSD [1] - [3]. The evolution of the PSD is governed by the interplay of three major phenomena, which are nucleation, growth and coagulation of the polymer particles. The interaction among these phenomena and the complexity of their relation to process variables (flowrates of the monomers, surfactant, and initiator) creates a challenging control problem. Another difficulty is that PSD measurements have significant measurement delays compared to the inherent time scale of the system.

Although the control of the emulsion polymerization systems is a well studied topic, see for example [4] - [6], typically involving the regulation of one or more of the lumped properties (*e.g.* moments of the distributions), the control of the distribution shape is largely an open problem. The indirect control of PSD through moments reduces the high dimensionality of the problem and results with suitable low-order systems for closed-loop control and dynamic optimization. However, for the cases where the desired distribution is complex, regulation of moments does not ensure the regulation to the target. Dynamic optimization has been applied extensively for obtaining an optimal batch recipe for emulsion polymerization as well as other PBE systems. Although the perfect execution of the nominal batch procedures would end with the desired distributions this is not always the case as the operation of emulsion polymerization systems are susceptible to various disturbances. Since the process is complex due to the interaction between growth, nucleation, and coagulation, most of the disturbances end up affecting the whole PSD. For example, any uncertainty in the rate of mechanical agitation, reactor temperature, and ingredient feed-rates would affect coagulation as well as the growth and the nucleation of the particles. In-batch feedback control of the distributions is needed for rejection of these disturbances ensuring consistent end-point PSDs for each batch.

In this work, an in-batch feedback control algorithm that controls the full PSD is presented. The algorithm uses a master controller to update the reference trajectories for the growth and nucleation kernels. The slave controller is designed to manipulate the feedrates of the monomers, surfactant, reducer, and oxidizer to keep the system following these updated trajectories. The cascade architecture enables the controller to exploit the relation

between the kernels better than a controller that would use the feedrates to the system as the manipulated variables. The algorithm is tested on a semibatch VAc/BuA emulsion copolymerization system where the evolution of the PSD is governed by a first order population balance equation (PBE). In the next section, the semibatch emulsion copolymerization system under study is presented. The following section outlines the controller algorithm. The paper is concluded with the results and discussion.

Semibatch VAc/BuA Emulsion Copolymerization System

In this study, a population balance equation (PBE) model, developed by Immanuel *et al.* [7] describing the evolution of the particle size distribution in a semibatch VAc/BuA copolymerization reactor is used as the plant. The model that is summarized in Table 1 consists of a PBE coupled with necessary mass balances. The model considers size dependent growth, partitioning of the nonionic surfactants, and the average number of radicals per particle calculations via first principles. A computationally efficient numerical method that exploits the different inherent time scales present in emulsion polymerization is used to solve the particle PBE, where the PSD is discretized into 250 finite elements of 2 nm width [8].

Table 1. PBE model for a semibatch emulsion copolymerization reactor

<i>Mass balance equations</i>	
Oxidizer	$d([I_w]V_{aq})/dt = -k_{d1}[I_w][Y_1^r] + v_{I_w}$
Reducer	$d([Y_2]V_{aq})/dt = -r_I k_{d1}[I_w][Y_1^r] + v_{Y_2}$
Initiator radical	$d([R_w]V_{aq})/dt = k_{d1}[I_w][Y_1^r] - V_{aq} \sum_{i=1}^2 k_{ri}[R_w][M_i]_w - V_{aq} k_{tav}^w [R_w] \left(\sum_{l=0}^{j_{cr}-1} [P_w]^l + [R_w] \right)$
Monomers	$\frac{dM_j}{dt} = v_{M_j} - \sum_{i=1}^2 (k_{pij}^w + k_{trij}^w) p_{wi} [P_w] [M_j]_w V_{aq} - \sum_{i=1}^2 (k_{pij} + k_{trij}) p_i [M_j]_p \int_{r_{nuc}}^{r_{max}} \bar{n}(r, t) F(r, t) dr$
<i>Population balance equation</i>	
Density function	$\frac{\partial}{\partial t} F(r, t) + \frac{\partial}{\partial r} (F(r, t) R_{growth}(r, t)) = R_{nuc}(r, t) + R_{coag}(r, t)$
Growth rate	$R_{growth}(r, t) = \frac{dr}{dt} = \frac{3}{4\pi r^2 \rho_p} \sum_{i=1}^2 \sum_{j=1}^2 k_{pij} p_i \frac{\bar{n}(r, t)}{N_A} [M_j]_p M W_j$
Nucleation rate	$R_{nuc} = R_{micellar} + R_{homo} = \sum_{l=0}^{j_{cr}-1} \sum_{i=1}^2 e_{i, micelle}^l p_{wi} [P_w]^l C_{micelle} V_{aq} + k_{pav}^w [P_w^{j_{cr}-1}] V_{aq}$
Coagulation rate	$R_{coag}(r, t) = H(r_{upper} - r) R_{formation}(r, t) - H(r_{cutoff} - r) R_{depletion}$ $R_{formation}(r, t) = \frac{1}{V_{aq}} \int \beta(r', r'') F(r', t) F(r'', t) \frac{r^2}{(r^3 - (r')^3)^{2/3}} dr'$ $R_{depletion}(r, t) = \frac{1}{V_{aq}} \int_{r_{nuc}}^{r_{max}} \beta(r, r') F(r, t) F(r', t) dr'$ where $\beta(r, r') = c_1 4\pi D_0 (r + r') / W_s$
<i>Output functions</i>	
Weight averaged PSD	$W(r_i, t) = r_i^3 F_i / \sum_i r_i^3 F_i$ where $F_i = \int_{r_{b, i-1}}^{r_{b, i}} F(r, t) dr$
Total particle number	$N_p = N_A \sum_i F_i$ Solid content $S_c = N_A \left(\sum_i 4\pi r_i^3 \rho_p F_i / 3 \right) / m_T$

The actual experimental system under consideration is presented in Fig. 1. The system consists of a 3L glass reactor, where the monomers, oxidizer, reducer, and the surfactant are delivered by remote setpoint metering pumps controlled by a digital control system. The PSD measurements can be obtained every 12 minutes by a capillary hydrodynamic fractionator (CHDF) with a measurement delay of 12 minutes and the density measurements are available every 1 minute from the on-line densitometer without delay. The semibatch system

runs under semibatch conditions and this allows for a monomer-starved operation, where there is no separate monomer phase is present. The initial conditions for the system and the manipulated variables of the slave controller with their base values are represented in Table 2.

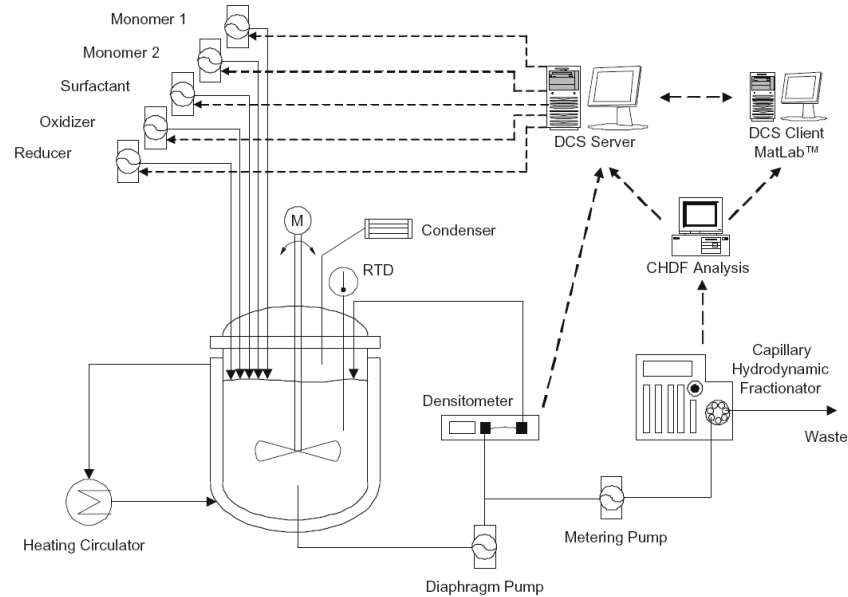


Figure 1. Schematic diagram of the simulated VAc/BuA emulsion copolymerization system.

Table 2. Semibatch VAc/BuA emulsion copolymerization system conditions

Initial Reactor Charge	
<i>Water</i>	1.0L
<i>VAc</i>	52g
<i>Ferrous ammonium sulphate</i>	0.1g
<i>Sodium benzoate</i>	1.12g
Reactor Temperature	
	67.5°C
System inputs	
	Base value of the input
<i>VAc</i> (u_1)	$0.299 \times 10^{-3} \text{ mol/s}$
<i>BuA</i> (u_2)	$0.281 \times 10^{-3} \text{ mol/s}$
<i>Surfactant</i> (u_3)	$0.710 \times 10^{-3} \text{ mol/s}$
<i>tBHP</i> (u_4)	$0.271 \times 10^{-3} \text{ mol/s}$
<i>SFS</i> (u_5)	$0.186 \times 10^{-3} \text{ mol/s}$

Cascade Control of Nucleation and Growth

The master controller for the regulation of the PSD uses the principal components of the PSD as the outputs and manipulates growth and nucleation variables. The growth variable that affects the growth kernel of the PBE is described as:

$$R_{growth} = \frac{M^w k_p p}{4\pi r^2 \rho_p N_A} C_p \quad (1)$$

where the vectors M^w , k_p , p , and C_p are the molecular weights, propagation constants, pseudo-homopolymer probabilities, and particle concentrations of the monomers, respectively. In Eq. 1, r is the particle size, ρ_p is the density of the particle phase, and N_A is the Avagadro's number. The nucleation variable is the nucleation kernel itself and is defined as:

$$R_{nuc} = \left(\sum_{l=0}^{j_{cr}-1} e^l p_w V_{aq} C_w^l C_{mic} \right) + \left(k_{Pav}^w V_{aq} C_w^{j_{cr}-1} \right) \quad (2)$$

where j_{cr} , e^l , p_w , V_{aq} , C_w^l , C_{mic} , k_{Pav}^w are the critical chain length for homogeneous nucleation, entry constant of oligo-radicals of length l into particles, aqueous pseudo-homopolymer probabilities, aqueous phase volume, aqueous concentration of oligomers of length l , concentration of micelles in the system, and average propagation kinetic constant for the water phase, respectively. These two variables act as the outputs for the slave controller of the cascade controller structure, as can be seen in Fig. 2. The slave controller uses the feedrates of monomers, surfactant, reducer, and the oxidizer to keep the nucleation and growth variables at their respective reference trajectories throughout the batch.

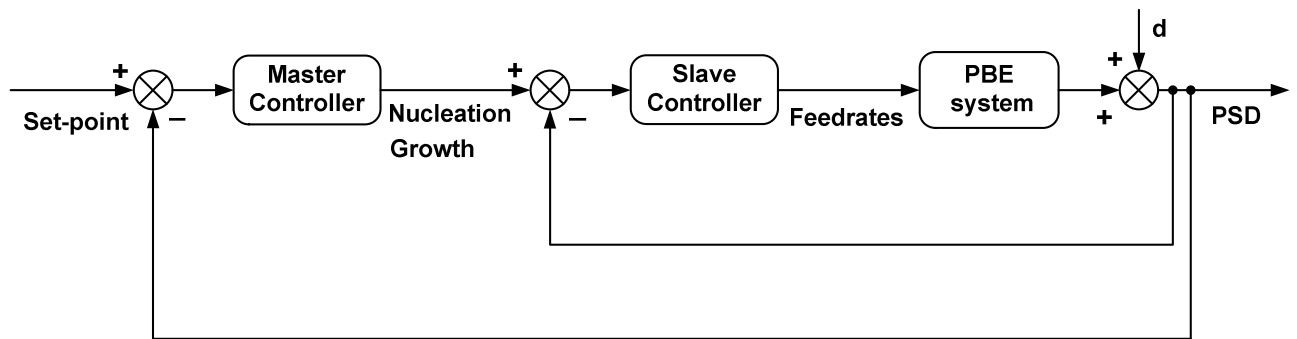


Figure 2. Proposed cascade algorithm for the regulation of PSD.

The primary controller is a nonlinear model predictive controller that uses the PBE model described in the previous section for the open-loop nonlinear predictions and the linearized version of the same model for predicting the effect of the manipulated variables on the system. As the effects of the inputs are incorporated linearly, the optimization problem for deciding on the future values of the inputs is a quadratic objective function that can be solved readily. The PBE model can be represented as a system of continuous-time nonlinear differential equations:

$$\begin{aligned} \dot{x} &= f(x, u) \\ y &= g(x) \end{aligned} \quad (3)$$

where x represents the system states and u represents manipulated variables. The discrete version of the model can be expressed as:

$$\begin{aligned} x_k &= F_{T_s}(x_{k-1}, u_{k-1}) \\ y_k &= g(x_k) \end{aligned} \quad (4)$$

where $F_{T_s}(x_{k-1}, u_{k-1})$ denotes the terminal vector obtained by integrating the continuous system equations one sampling time, T_s , from the initial state vector, x_{k-1} , holding the manipulated variable, u_{k-1} , constant. After augmenting the model states with the plant outputs, and delayed outputs the state evolution equation is obtained as:

$$\begin{aligned} \underbrace{\begin{bmatrix} x_k \\ y_k^c \\ y_k^{c\theta} \end{bmatrix}}_{\bar{X}_k} &= \underbrace{\begin{bmatrix} F_{T_s}(x_{k-1}, u_{k-1}) \\ g(F_{T_s}(x_{k-1}, u_{k-1})) \\ y_{k-\theta}^c \end{bmatrix}}_{\Phi(x_{k-1}, u_{k-1})} + \underbrace{\begin{bmatrix} B^d \\ 0 \\ 0 \end{bmatrix}}_{\Gamma^d} d_{k-1} \\ \hat{Y}_k &= \underbrace{\begin{bmatrix} 0 & 0 & I \end{bmatrix}}_{\Xi_k} \bar{X}_k + v_k \end{aligned} \quad (5)$$

First, model prediction is performed by integrating the nonlinear model one time step with the information at time step $k-1$ and then the state vector is corrected with the current measurement vector using the optimal Kalman gain assuming, d and v are white noises with covariances Q_d and R :

$$\begin{aligned} \bar{X}_{k|k-1} &= \Phi(x_{k-1}, u_{k-1}) \\ \bar{X}_{k|k} &= \bar{X}_{k|k-1} + K_{f,k} \left(\hat{Y}_{k,meas.} - \Xi_k \bar{X}_{k|k-1} \right) \end{aligned} \quad (6)$$

where the Kalman gain is computed using the linearized plant at time $k-1$. This linear system can be represented as:

$$\underbrace{\begin{bmatrix} x_k \\ y_k^c \\ y_k^{c\theta} \end{bmatrix}}_{\bar{X}_k} = \underbrace{\begin{bmatrix} A_{k-1} & 0 & 0 \\ C_{k-1}A_{k-1} & 0 & 0 \\ 0 & I & 0 \end{bmatrix}}_{\Phi_{lin}(x_{k-1}, u_{k-1})} \underbrace{\begin{bmatrix} x_{k-1} \\ y_{k-1}^c \\ y_{k-1}^{c\theta} \end{bmatrix}}_{\bar{X}_{k-1}} + \underbrace{\begin{bmatrix} B_{k-1}^u \\ C_{k-1}B_{k-1}^u \\ 0 \end{bmatrix}}_{\Gamma_{k-1}^u} u_{k-1} + \underbrace{\begin{bmatrix} B_{k-1}^d \\ C_{k-1}B_{k-1}^d \\ 0 \end{bmatrix}}_{\Gamma_{k-1}^d} d_{k-1} \quad (7)$$

$$\hat{Y}_k = \underbrace{\begin{bmatrix} 0 & 0 & I \end{bmatrix}}_{\Xi_k} \bar{X}_k + v_k$$

The Kalman gain, $K_{f,k}$, and the state covariance, P_k , are updated as:

$$P_{k|k-1} = (\Phi_{k-1}^{lin.}) P_{k-1|k-1} (\Phi_{k-1}^{lin.})^T + Q_{d_k}$$

$$K_{f,k} = P_{k|k-1} (\Xi_k)^T \left[(\Xi_k) P_{k|k-1} (\Xi_k)^T + R_k \right]^{-1} \quad (8)$$

$$P_{k|k} = (I - K_{f,k} \Xi_k) P_{k|k-1}$$

for which the initial covariance of the state vector, P_0 , is defined appropriately. The multistep-ahead MPC prediction equation is formulated such that the contribution of the future unknown input changes on the controlled outputs is linear. The prediction equation can be expressed as:

$$Y_{k+1|k}^c = S^x + S^u \Delta U_k \quad (9)$$

where

$$Y_{k+1|k}^c = \begin{bmatrix} \hat{Y}_{k+1|k} \\ \hat{Y}_{k+2|k} \\ \vdots \\ \hat{Y}_{k+p|k} \end{bmatrix} \quad \Delta U_k = \begin{bmatrix} \Delta u_k \\ \Delta u_{k+1} \\ \vdots \\ \Delta u_{k+q-1} \end{bmatrix} \quad S^u = \begin{bmatrix} C_k^c B_k^u & 0 & \cdots & 0 \\ C_k^c (I + A_k) B_k^u & C_k^c B_k^u & \cdots & 0 \\ \vdots & \vdots & \ddots & \vdots \\ C_k^c \sum_{i=0}^{p-1} A_k^i B_k^u & C_k^c \sum_{i=0}^{p-2} A_k^i B_k^u & \cdots & C_k^c \sum_{i=0}^{p-q} A_k^i B_k^u \end{bmatrix}$$

$$S^x = \begin{bmatrix} g(F_{T_s}(x_{k|k}, u_{k-1})) - y_k^{nom.} \\ g(F_{2,T_s}(x_{k|k}, u_{k-1})) - y_{k+1}^{nom.} \\ \vdots \\ g(F_{p,T_s}(x_{k|k}, u_{k-1})) - y_{k+p}^{nom.} \end{bmatrix}$$

The computation of the optimal control input is established by formulating and solving a quadratic program that can be solved by a suitable quadratic programming (QP) solver:

$$\begin{aligned}
& \min_{U_k} \left\| \Lambda^y (Y_{k+1|k}^c - R_{k+1|k}) \right\|_2^2 + \left\| \Lambda^u \Delta U_k \right\|_2^2 \\
& \text{s.t.} \quad U_L \leq U_k \leq U_U \\
& \quad \quad \quad |\Delta U_k| \leq \Delta U_{max}
\end{aligned} \tag{10}$$

In a similar but more direct approach, the linearization of the nonlinear plant model is avoided and a nonlinear constrained optimization problem is formulated to obtain the future manipulated variable changes. The nonlinear optimization problem is formulated as:

$$\begin{aligned}
& \min_{U_k} \left\| \Lambda^y (y_{k+p|k} - y_{k+p}^{nom.}) \right\|_2^2 \\
& \text{s.t.} \quad U_L \leq U_k \leq U_U \\
& \quad \quad \quad |\Delta U_k| \leq \Delta U_{max}
\end{aligned} \tag{11}$$

where $y_{k+p|k}$ is defined as the last element of the vector:

$$Y_{k+1|k} = \begin{bmatrix} g \left(F_{T_s} (x_{k|k}, u_{k|k}) \right) - y_k^{nom.} \\ g \left(F_{T_s} (x_{k+1|k}, u_{k+1|k}) \right) - y_{k+1}^{nom.} \\ \vdots \\ g \left(F_{T_s} (x_{k+p|k}, u_{k+p|k}) \right) - y_{k+p}^{nom.} \end{bmatrix} \tag{12}$$

It must be noted that the nonlinear plant model is used for the closed-loop prediction of the controlled outputs in Eq. 11. This is different from Eq. 9, where the nonlinear plant model is only used for the open-loop prediction of the outputs. Also, a nonlinear programming (NLP) solver should be used for the optimization problem described in Eq. 11.

The discrete system matrices at time, k , are obtained by linearization around a nominal point and application of a zero order hold. As this linearization yields a high order model (258 states, 250 outputs) that is ill-conditioned, model order reduction is accomplished using principal component analysis (PCA). The reduced states, x , and the reduced outputs, y^c , are obtained from the normalized original states, \tilde{x} , and normalized original outputs \tilde{y}^c by the orthonormal linear transformation matrices, P_k^x and P_k^y :

$$\begin{aligned}
x_k &= (P_k^x)^T \tilde{x}_k \\
y_k^c &= (P_k^y)^T \tilde{y}_k^c
\end{aligned} \tag{10}$$

with this transformation, the reduced order system matrices are:

$$A_k = (P_k^x)^T \tilde{A}_k (P_k^x) \quad B_k^u = (P_k^x)^T \tilde{B}_k^u \quad C_k = (P_k^x)^T \tilde{C}_k (P_k^y)^T \tag{11}$$

where \tilde{A}_k , \tilde{B}_k^u , and \tilde{C}_k are the full order state matrices at time k . The distributed states (\tilde{x} that represents F), discretized population density function in Table 1, and the outputs, (\tilde{y}^c that represents $wPSD$) have different PCA models for each time point throughout the batch. The training data for the PCA models consists of 60 batches and the model construction from this multiway data is presented in Fig. 3.

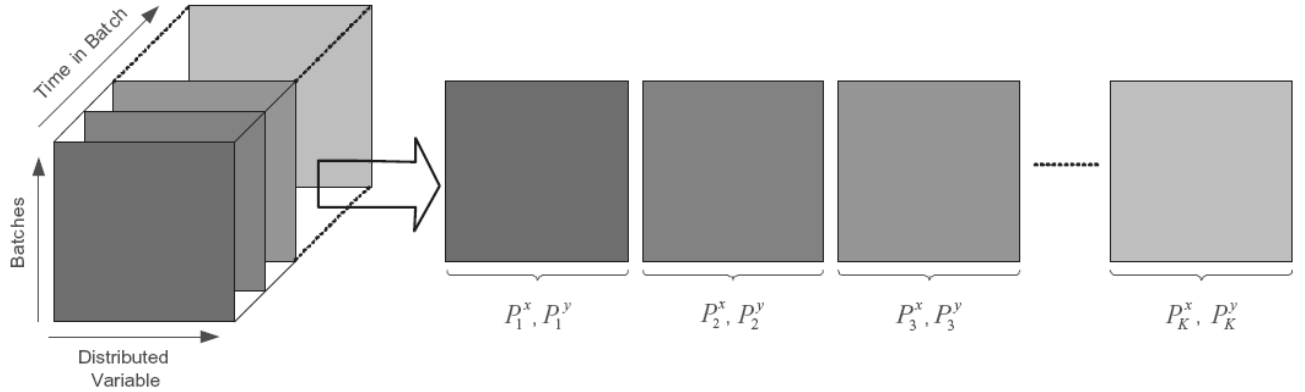


Figure 3. Unfolding of the multiway data applied in this work. At each discrete time point (every 1 minute) a PCA models for the population density and $wPSD$ are constructed using a training database of 60 batches.

Results and Discussion

The proposed controller with the objective function defined in Eq. 10 was tested against a disturbance in the initial VAc amount inside the reactor, where the initial VAc inside the reactor was 100% higher than its nominal amount. The PSD measurements are obtained by the master controller every 12 minutes with 12 minutes of delay. With the information of PSD the master controller computes the change of growth and nucleation variables that are imposed on their nominal trajectories. The perfect slave controller considered for this case ensures that growth and nucleation follows their updated trajectories. The resulting $wPSDs$ for the controlled, uncontrolled, and the nominal cases are presented in Fig. 4. The

uncontrolled distribution has a lower secondary peak due to lower micellar nucleation events and a shifted primary peak due to slow growth of the larger particles caused by the higher VAc inside the system. The controlled distribution shows that the controller was able to regulate both peaks as both the amplitudes and positions are moved towards the target distribution. The controlled distribution was 98% closer to the target distribution compared to the uncontrolled distribution (computed as,

$$(\|wPSD_{uncontr} - wPSD_{nom}\| - \|wPSD_{contr} - wPSD_{nom}\|) / \|wPSD_{uncontr} - wPSD_{nom}\|).$$

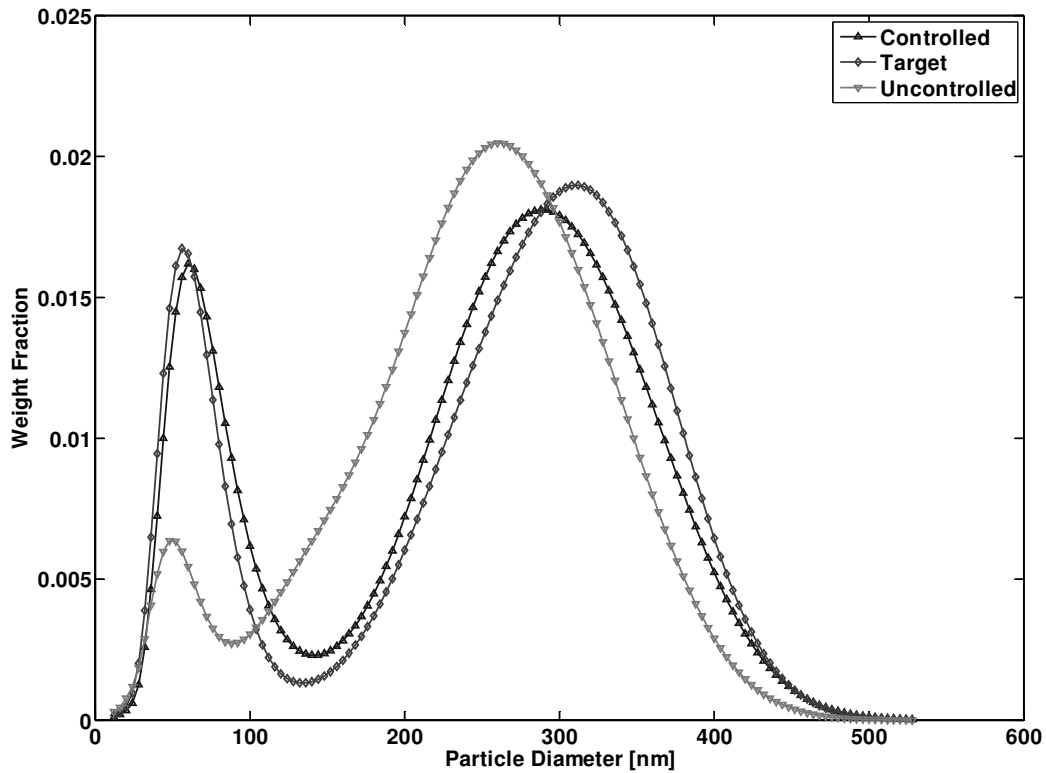


Figure 4. Controlled, target, and uncontrolled wPSDs in the case of a 100% higher initial VAc holdup in the reactor.

The nominal and the updated trajectories of the nucleation and growth variables are presented in Fig. 5. The nucleation is increased as the disturbance on the system suppresses the micellar nucleation events and would result with a smaller secondary peak if not regulated. The growth is also increased that helps regulate the primary peak of the wPSD to its target. It must be noted that no corrective action is employed by the controller until the first wPSD measurement is available.

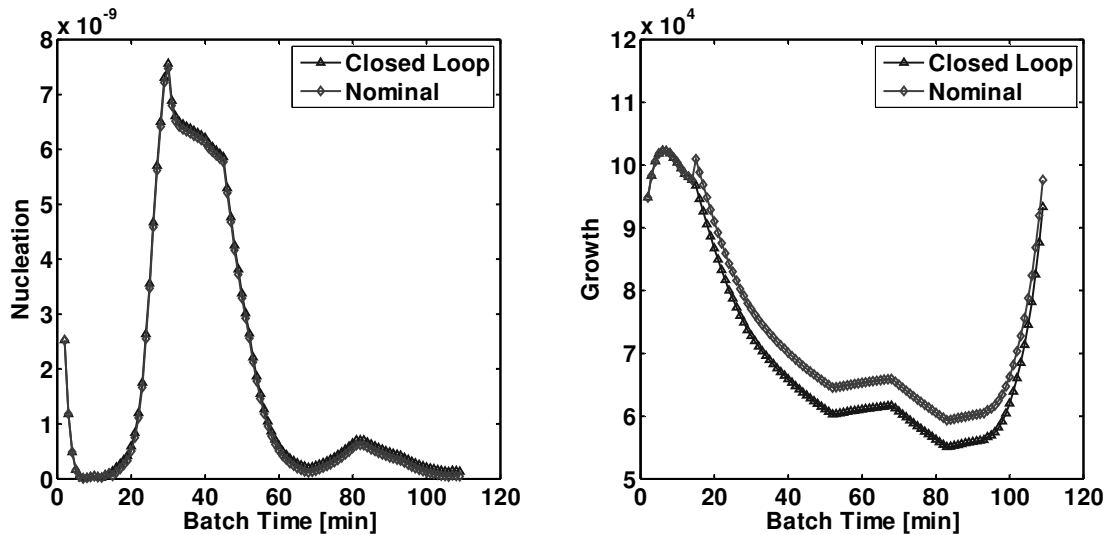


Figure 5. Closed loop and the nominal trajectories of the manipulated variables for the 100% higher initial VAc disturbance.

The controller with the objective function defined in Eq. 11 was tested against a disturbance, where the growth rate was lowered by 80% of its nominal value for the first 14 minutes of the batch. As in the previous disturbance scenario a perfect slave controller was considered for the system after the 14th minute of the batch. Also, in this case the states of the were assumed to be measured by the controller. The sequential quadratic programming (SQP) solver of MATLAB, `fmincon`, was used as the NLP solver. Controlled, uncontrolled, and the nominal wPSDs for this disturbance case are presented in Fig. 6. The uncontrolled distribution is largely affected by the disturbance as evident by the disturbed primary and secondary peaks. However, the controller adjusts the nucleation and growth, as seen in Fig. 7, accordingly to reject the disturbance and the controlled distribution is moved to the target. It can be seen that the controller increases the growth to compensate for the reduced growth and nucleation is lowered immediately to correct for the increased secondary peak amplitude as soon as the first measurement is available. In this case, the controlled distribution was 78% closer to the target distribution compared to the uncontrolled distribution.

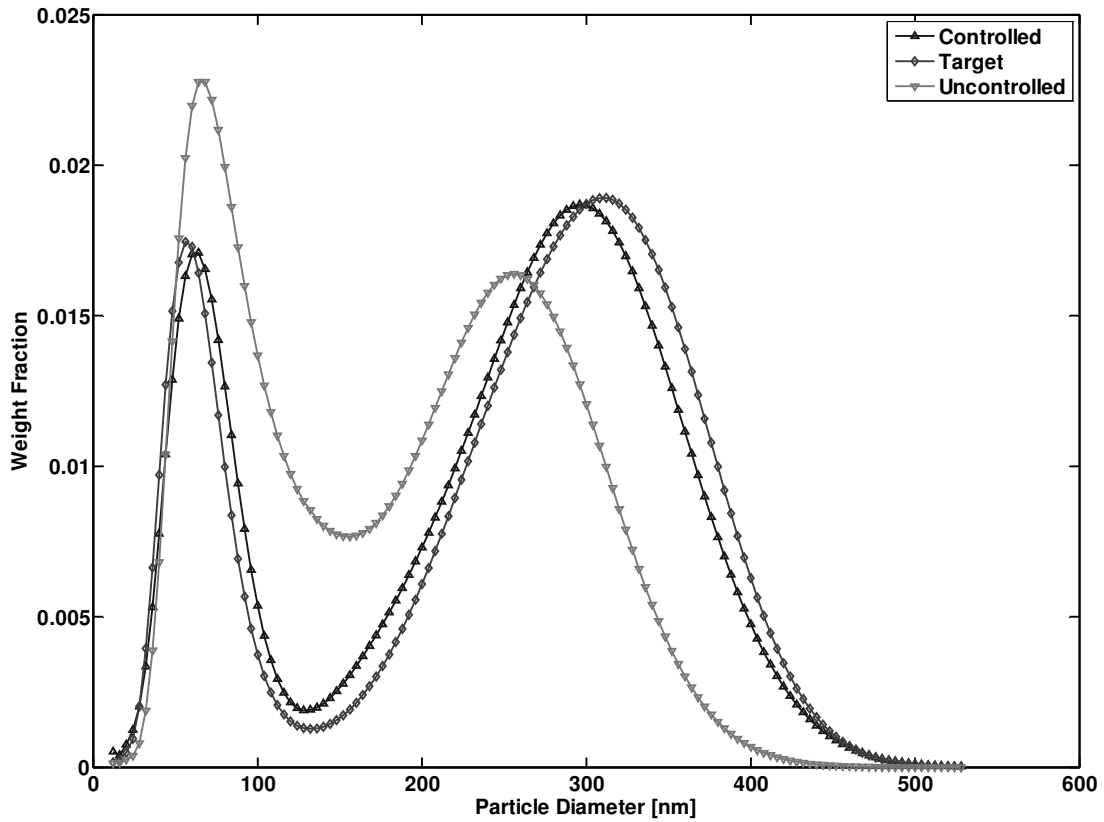


Figure 6. Controlled, target, and uncontrolled wPSDs in the case of a 80% lowered growth rate with respect to the nominal case for the first 14 minutes of the batch.

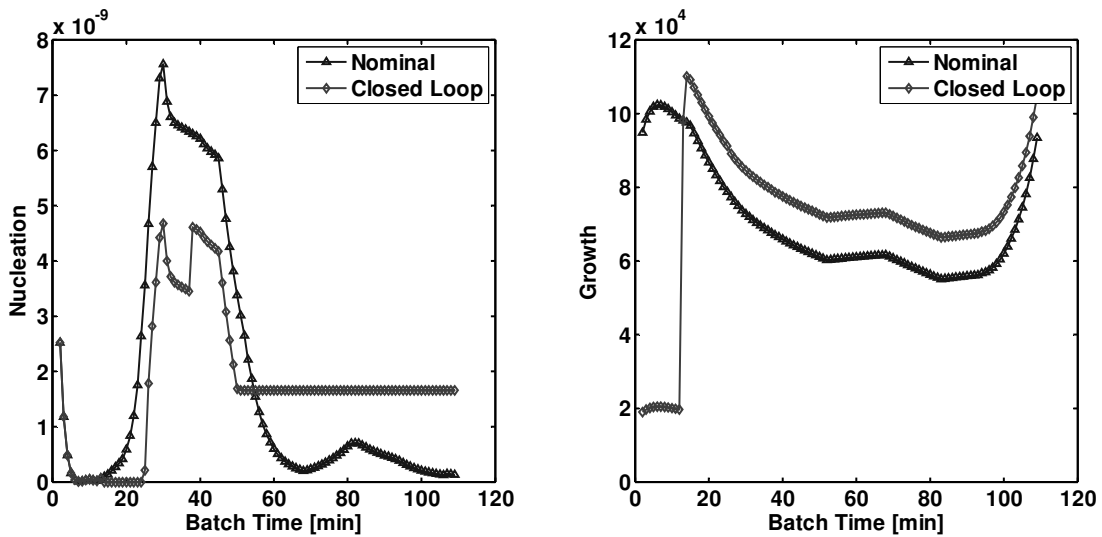


Figure 7. Closed loop and the nominal trajectories of the manipulated variables for the disturbance of a 80% lowered growth rate for the first 14 minutes of the batch.

Summary

A cascade approach, where the nucleation and growth events are manipulated by a master controller is developed for the regulation of the full PSD in a semibatch emulsion copolymerization system. In this approach a slave controller is manipulating the feedrates to the system in order to attain the updated trajectories of growth and nucleation by a master controller. The master controller uses PCA based model order reduction for the high dimensional distributed outputs and states of the system. The controller's performance was tested against a large disturbance of 100% higher initial VAc amount and another disturbance of 80% lowered growth for the first 14 minutes and was found to be satisfactory. Although the model system used in this work was governed by a first order PBE, presented methods are applicable to other PBE systems where the nucleation and growth are the dominant mechanisms determining the shape of the PSD.

References

1. J. R. Richards and J. P. Congalidis. Measurement and control of polymerization reactors. In *Proceedings of the Seventh International Conference on Chemical Process Control*, Alberta, Canada, 2006.
2. M. Do Amaral, S. Van Es, and J. M. Asua. Effect of the particle size distribution on the low shear viscosity of high-solid-content latexes. *J. Polym. Sci., Part A: Polym. Chem.*, 42:3936-3946, 2004.
3. J. Dimitratos, G. Elicabe, and C. Georgakis. Control of emulsion polymerization reactors. *AIChE J.*, 40:1993-2021, 1994.
4. D. Shi, N. H. El-Farra, M. Li, P. Mhaskar, and P. D. Christofides. Predictive control of particle size distribution in particulate processes. *Chem. Eng. Sci.*, 61:268-281, 2006.
5. B. Alhamad, J. A. Romagnoli, and V. G. Gomes. On-line multi-variable predictive control of molar mass and particle size distributions in free radical emulsion polymerization. *Chem. Eng. Sci.*, 60:6596-6606, 2005.
6. R. Gesthuisen, S. Kramer, and S. Engell. Hierarchical control scheme for time-optimal operation of semibatch emulsion polymerizations. *Ind. Eng. Chem. Res.*, 43:7410-7427, 2004.
7. C. D. Immanuel, C. F. Cordeiro, S. S. Sundaram, E. S. Meadows, T. J. Crowley, and F. J. Doyle III. Modeling of Particle Size Distribution in Emulsion Co-Polymerization: Comparison with Experimental Data and Parametric Sensitivity Studies. *Comput. Chem. Eng.*, 26: 1133-1152, 2002.
8. C. D. Immanuel and F. J. Doyle III. Computationally efficient solution of population balance models incorporating nucleation, growth and coagulation: application to emulsion polymerization. *Chem. Eng. Sci.*, 58:3681-3698, 2003.